

Reaction $^{40}\text{Ar}(p, n)$ to the Antianalog State in $^{40}\text{K}^\dagger$

Aaron Galonsky, J. G. Branson,* R. R. Doering, and D. M. Patterson†

Cyclotron Laboratory, Department of Physics, Michigan State University, East Lansing, Michigan 48824

(Received 1 November 1973; revised manuscript received 14 August 1975)

We have measured $^{40}\text{Ar}(p, n)^{40}\text{K}(\text{antianalog})$ differential cross sections at 24 MeV and made microscopic distorted-wave Born-approximation calculations for these cross sections. Unlike the $(^3\text{He}, t)$ reaction to the same state, where it is necessary to invoke a two-step mechanism, the (p, n) data are fitted by the one-step calculation. A one-step calculation also fits $^{40}\text{Ar}(p, n)^{40}\text{K}(\text{isobaric analog})$ data with the same nucleon-nucleon interaction used in the antianalog-state calculation.

Just as a transition to the isobaric analog state (IAS) of a target is strong and insensitive to details because of the near-perfect overlap of target and IAS wave functions, a transition to the antianalog state (AAS) may be expected to be small and sensitive to details because of the almost complete orthogonality of target and AAS wave functions. This sensitivity has been seen in $(^3\text{He}, t)$ reactions to the AAS in several nuclei, where it was found that the $L=0$ angular distributions expected of $0^+ \rightarrow 0^+$ transitions were not observed.¹ Cross sections for $^{40}\text{Ar}(^3\text{He}, t)^{40}\text{K}(\text{AAS})$ computed by Schaeffer and Bertsch² with the direct microscopic model were one to two orders of magnitude below the observed values, but a reasonable fit was obtained when the two-step pickup-stripping process $(^3\text{He}, \alpha)-(\alpha, t)$ was included.² The data and calculations are shown in Fig. 1. Similar results were obtained by Coker, Udegawa, and Wolter³ who fitted both 35-MeV¹ and 18-MeV⁴ data. Experimental discrepancies with expected shapes of angular distributions have also been noted when the transferred L was greater than 0.⁵ For the reaction $^{48}\text{Ca}(^3\text{He}, t)^{48}\text{Sc}$, two-step calculations using $(^3\text{He}, \alpha)-(\alpha, t)$ ^{2,6} or, in addition, $(^3\text{He}, d)-(d, t)$ ⁷ have produced fits to data where one-step calculations clearly disagreed with experiment. It seems well documented that a reaction mechanism including two-step amplitudes is needed to describe $(^3\text{He}, t)$ reactions.

In order to test for the presence of a two-step amplitude in (p, n) reactions, we have investigated the reaction $^{40}\text{Ar}(p, n)^{40}\text{K}(\text{AAS})$ with 24-MeV protons. As for $(^3\text{He}, t)$ reactions to the AAS, the near orthogonality of the target and final-state wave functions should produce small one-step (p, n) amplitudes, thus allowing us to see in the AAS transition a two-step amplitude which might be masked in the IAS transition.

Neutrons were detected with a liquid-scintilla-

tor, time-of-flight spectrometer⁸ having an instrumental resolution of ~ 0.5 nsec. To achieve an energy resolution sufficient to resolve cleanly the AAS neutron group [$E_x(^{40}\text{K}) = 1.64$ MeV] from the stronger group at 1.96 MeV, flight paths were increased from our normal value of ~ 4.5 m to 11–15 m. At these flight paths the geometry of our laboratory permitted neutrons to be observed only in the angular ranges $10\text{--}35^\circ$ and $135\text{--}152^\circ$. It would be best to resolve the AAS and measure its cross section at all angles. However, it will be seen that the information obtained at this combination of forward and backward angles is sufficient to conclude that a significant two-step

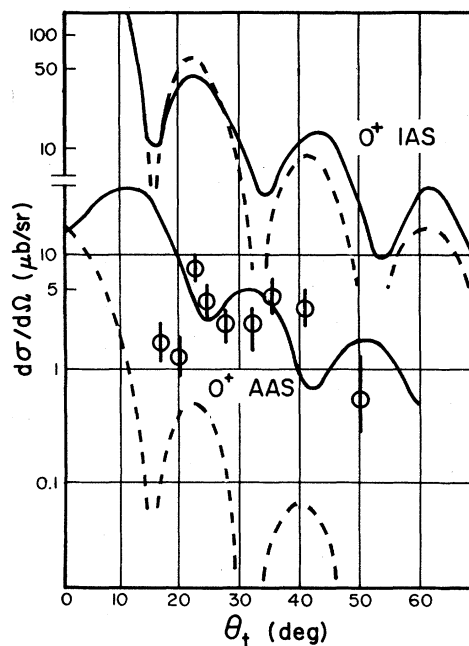


FIG. 1. Comparison of the one-step (dashed curves) and the one-step-plus-two-step (solid curves) calculations of Ref. 2 with the data of Ref. 1 for the reaction $^{40}\text{Ar}(^3\text{He}, t)^{40}\text{K}$ to the IAS and the AAS.

(p, n) amplitude is not required.

The targets were gas cells with entrance and exit windows of 2-mil aluminum foil. For the forward angles the cell was 2.54 cm long with a pressure of 1.8 atm. The neutron energy resolution at the AAS computed and observed in the spectra was ~ 0.18 MeV. One spectrum is shown in Fig. 2. According to the known energies of ^{40}K states,⁹ the nearest neighbor to the AAS is the 1.96-MeV state, from which the AAS is adequately resolved. Other peaks in the spectrum may arise from excitation of doublets or clusters of states. The twin peaks labeled Al windows in Fig. 2 arise from the ground-state transition in the aluminum entrance (right-hand peak) and exit (left-hand peak) windows. The centroids of these peaks are separated by an amount corresponding to the sum of the proton energy losses in one half the entrance window, the argon gas target, and one half the exit window. For the backward angles a shorter cell, 1.1 cm long, was used with a higher pressure, 3.7 atm. The smaller cell length was necessary because neutrons produced near the back of the cell, i.e., by protons of degraded energy, have less energy and also have a longer flight path than neutrons produced

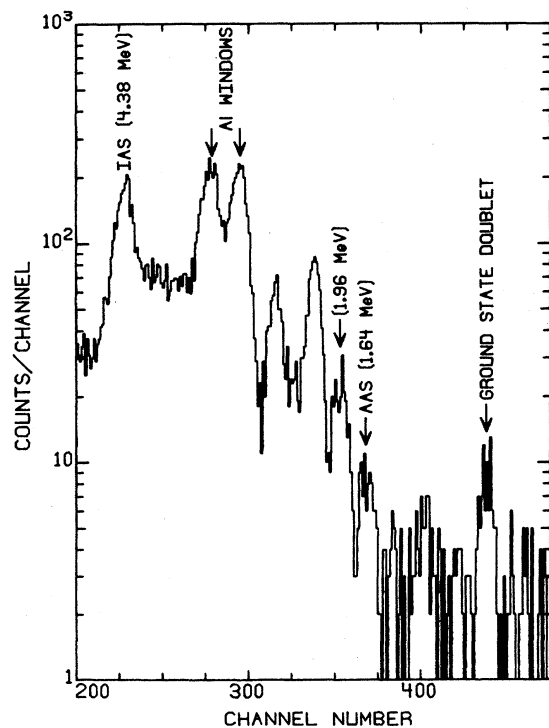


FIG. 2. Neutron time-of-flight spectrum at 15° for 24-MeV protons on ^{40}Ar .

at the entrance to the cell. Hence, contributions to the resolution from cell length and from dE/dx are additive at backward angles. The computed detection efficiencies were about 3%.¹⁰

Our AAS cross sections at 24.0 MeV and the IAS cross sections of Bentley *et al.*¹¹ at 22.8 MeV are plotted in Fig. 3. The curves in Fig. 3 are the results of one-step microscopic calculations with the distorted-wave code DWBA-70 of Raynal and Schaeffer.¹² In this code both the direct and knock-on-exchange amplitudes are included in the computation. The dashed curves in the figure are for direct only; the solid curves include exchange. The ^{40}Ar neutron-excess wave function was taken as a pure $d_{3/2}^2 f_{7/2}^2$ configuration. All bound-state wave functions were derived from a Woods-Saxon potential with radius parameter 1.25 fm, diffuseness 0.65 fm, and spin-orbit strength 6 MeV. Binding energies of the orbitals

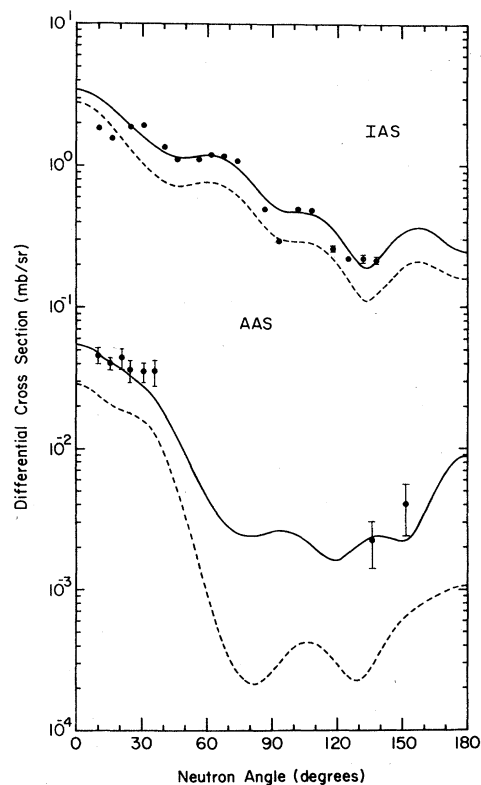


FIG. 3. $^{40}\text{Ar}(p, n)^{40}\text{K}$ cross sections to the IAS (at 22.8 MeV) and AAS (at 24.0 MeV) of the target. The IAS data are taken from Ref. 11. The curves are from distorted-wave Born-approximation one-step microscopic calculations made under conditions described in the text. The dashed curves are for the direct transition only; the solid curves have both the direct and the knock-on-exchange contributions.

in ^{40}Ar , $^{40}\text{K}(\text{IAS})$, and $^{40}\text{K}(\text{AAS})$ were obtained from the separation energy of a neutron from ^{40}Ar , the $f_{7/2}$ and $d_{3/2}$ hole states in ^{39}Ar , the Coulomb displacement energy, and the IAS-AAS splitting in ^{40}K . Proton and neutron optical-model parameters had the "best-fit" values of Becchetti and Greenlees.¹³ The nucleon-nucleon effective interaction had the shape of a single Yukawa potential with range 1.0 fm and strengths with the phenomenological values of $V_0 = -27$ MeV and $V_{\sigma\tau} = 12$ MeV; neither V_σ nor V_τ was fixed by Austin's phenomenological survey.¹⁴ For V_σ we used the Kallio-Kolltveit G -matrix value,¹⁵ 6.5 MeV, and for V_τ we used 20 MeV.¹⁶ If accompanied by modest changes in V_τ , no reasonable variation in the other force parameters, in the optical-model parameters, or in the nuclear wave functions could substantially change the calculated angular distributions.

Although the calculations in Fig. 3 give too steep a rise in the IAS cross sections near 0° , the agreement between theory and experiment is otherwise very good. Even the very small AAS cross sections predicted for backward angles is verified by our two measurements at 135° and 152° . At these angles the AAS cross sections are only 1% of the IAS cross sections. Any sizable two-step process could only fortuitously permit such small cross sections to occur.

The good fit to the AAS (p, n) data, in contrast to the very large discrepancies found between theory and experiment in the $(^3\text{He}, t)$ reaction (see Fig. 1), indicates that the use of multistep processes is not presently called for in the interpretation of (p, n) reactions. Perhaps it is to be expected that multistep processes should be much more significant when the initial and final particles are composites of nucleons, for which the direct cross sections are generally very small.

$^{56}\text{Fe}(p, n)^{56}\text{Co}(\text{AAS})$ data have been fitted by including a (p, d) - (d, n) two-step amplitude.¹⁷ Beyond 20° , where the cross sections are less than 0.01 mb/sr, most of the data may be questioned because Gaussian unfolding procedures were necessary to extract the AAS peak area from that of a stronger neighboring peak. Furthermore, the calculations did not include the knock-on exchange. Instead, it was assumed that exchange would not change the shape of either the IAS or AAS angular distribution, and that, in magnitude, exchange would have the same effect on both transitions. From Fig. 3 we can see that these assumptions were not valid. Knock-on exchange

greatly reduces the anisotropy of the AAS angular distribution. Finally, the validity of some approximations in (p, d) - (d, n) calculations is not clear; neglected finite-range corrections, in particular, may be very important.¹⁸

Although we have demonstrated with only one case the adequacy of a one-step treatment for the (p, n) reaction, this conclusion may be true in general because the case chosen has an intrinsically small one-step cross section and is therefore sensitive to the display of multistep processes.

We would like to thank Professor H. McManus and Professor G. F. Bertsch for useful discussions and for help in using DWBA-70 for (p, n) reactions.

†Work supported by the National Science Foundation and the U. S. Office of Naval Research.

*Present address: Princeton University, Princeton, N. J. 08540.

‡Present address: University of Texas, Austin, Tex. 78712.

¹R. A. Hinrichs, R. Sherr, G. M. Crawley, and I. Proctor, Phys. Rev. Lett. **24**, 829 (1970).

²R. Schaeffer and G. F. Bertsch, Phys. Lett. **38B**, 159 (1972).

³W. R. Coker, T. Udegawa, and H. H. Wolter, Phys. Lett. **41B**, 237 (1972).

⁴J. J. Wesolowski, L. F. Hansen, and M. L. Stelts, Phys. Rev. **172**, 1072 (1968).

⁵P. Kossanyi-Demay, P. Roussel, H. Farraggi, and R. Schaeffer, Nucl. Phys. **A148**, 181 (1970); J. R. Comfort, J. P. Schiffer, A. Richter, and M. M. Stautberg, Phys. Rev. Lett. **26**, 1338 (1971); R. A. Hinrichs and G. F. Trentelman, Phys. Rev. C **4**, 2079 (1971).

⁶M. Toyama, Phys. Lett. **38B**, 147 (1972).

⁷N. B. deTakacsy, Phys. Lett. **42B**, 1 (1972).

⁸R. St. Onge, Aaron Galonsky, R. K. Jolly, and T. M. Amos, Nucl. Instrum. Methods **126**, 391 (1975); R. R. Doering, D. M. Patterson, and Aaron Galonsky, Phys. Rev. C **12**, 378 (1975).

⁹P. M. Endt and C. Van Der Leun, Nucl. Phys. **A105**, 1 (1967).

¹⁰Computed with the code described by R. J. Kurz, Lawrence Radiation Laboratory Report No. UCRL 11339, 1964 (unpublished).

¹¹R. F. Bentley, J. D. Carlson, D. A. Lind, R. B. Perkins, and C. D. Zafiratos, Phys. Rev. Lett. **27**, 1081 (1971), and private communication.

¹²We are grateful to Dr. Schaeffer for bringing DWBA-70 to our laboratory during a visit in 1971.

¹³F. S. Becchetti, Jr., and G. W. Greenlees, Phys. Rev. **182**, 1190 (1969).

¹⁴S. M. Austin, in *The Two-Body Force in Nuclei*, edited by S. M. Austin and G. M. Crawley (Plenum, New York, 1972), p.285.

¹⁵F. Petrovich, H. McManus, V. A. Madsen, and

J. Atkinson, Phys. Rev. Lett. **22**, 895 (1969).

¹⁶F. Petrovich, Ph.D. thesis, Michigan State University, 1970 (unpublished). In a survey of five realistic interactions V_τ ranged from a 17.8 to 21 MeV.

¹⁷H. W. Fielding, L. D. Rickertsen, P. D. Kunz, D. A.

Lind, and C. D. Zafiratos, Phys. Rev. Lett. **33**, 226 (1974).

¹⁸P. D. Kunz and L. D. Rickertsen, Bull. Am. Phys. Soc. **20**, 666 (1975); L. D. Rickertsen, private communication.

Quasiparticle Pole Strength in Nuclear Matter*

R. S. Poggioli

Department of Physics and Astronomy, University of Maryland, College Park, Maryland 20742

and

A. D. Jackson

Department of Physics, State University of New York, Stony Brook, New York 11790

(Received 18 August 1975)

It is argued that single-particle-like behavior in nuclear matter is much less probable than Brueckner theory suggests. In particular, the quasiparticle pole strength is evaluated for nuclear matter and it is shown that, contrary to the spirit of Brueckner theory, low-momentum states play a crucial role in determining the magnitude of z_{k_F} .

In Brueckner theory, the probability that nuclear matter cannot be described adequately in terms of single-particle-like behavior is given by κ , Brandow's defect-wave-function probability.¹ Earlier calculations have estimated $\kappa \approx 0.20$. The smallness of κ is usually offered as an explanation for the success of the independent-particle (shell) model of nuclei. Unfortunately, all previous calculations of κ have assumed that high-momentum states alone provide the dominant contribution. While this is certainly true for the ground-state energy, the authors have shown in an earlier paper² that many other properties of nuclear matter are strongly affected by contributions from low-lying states. In the present paper, it will be shown that these low-lying states have a pronounced effect on single-particle-like behavior, making it much less probable.

Let us begin with a brief review of the pertinent concepts of Brueckner theory: Since the internucleon force is short ranged, two-body scattering dominates. Since the nuclear force is strong, high-momentum particle states dominate because of their clear phase-space advantage (over hole states, in particular). The appropriate, correlated two-body wave function is

$$\Psi = \Phi - (Q/e)V\Psi \quad (1)$$

in which Φ is the uncorrelated wave function and the Pauli operator Q excludes hole states. This equation becomes identical to the free scattering equation if the Pauli operator is replaced by un-

ity. In this case, the zero in the energy denominator, corresponding to energy conservation, leads to the outgoing scattered wave. In Eq. (1), however, the Pauli operator prevents the energy denominator from vanishing. Hence, there can be no real (energy conserving) scattering and, at sufficiently large distances, the correlated wave function must approach the uncorrelated wave function or, equivalently, the defect wave function

$$\xi = \Phi - \Psi$$

must vanish. This is the chief effect which the presence of the other particles (the Fermi sea) has on the two scattering particles. In nuclear matter, Ψ approaches the uncorrelated plane wave very rapidly; this phenomenon is called "healing."³ At extremely small distances, the core region of the internucleon potential makes Ψ negligibly small, thus producing a "wound" in the wave function; however, this wound heals very rapidly. In other words, $|\xi(\vec{r})|$ is approximately unity in the core region where the particles are strongly correlated and goes rapidly to zero as r increases. It is useful to define the range d of the two-body correlations by

$$\frac{4}{3}\pi d^3 = \int |\xi(\vec{r})|^2 d^3r. \quad (2)$$

This distance should be compared with the average interparticle spacing r_0 defined by

$$\frac{4}{3}\pi r_0^3 = n^{-1} \quad (3)$$